Proc. Natl. Acad. Sci. USA
Vol. 92, pp. 1082–1086, February 1995
Biophysics

Internal and interfacial dielectric properties of cytochrome *c* from molecular dynamics in aqueous solution

THOMAS SIMONSON*† AND DAVID PERAHIA‡

*Laboratoire de Biologie Structurale, Centre National de la Recherche Scientifique, Institut de Génétique et Biologie Moléculaire et Cellulaire, BP 163, Communauté Urbaine de Strasbourg, 67404 Illkirch, France; and ‡Laboratoire d'Enzymologie Physico-Chimique et Moléculaire, Université de Paris-Sud, 91405 Orsay, France

Communicated by Frederic M. Richards, Yale University, New Haven, CT, October 24, 1994 (received for review April 5, 1994)

ABSTRACT **The dielectric properties of proteins are central to their stability and activity. We use the Fröhlich–Kirkwood theory of dielectrics to analyze two 1-ns molecular dynamics simulations of ferro- and ferricytochrome *c* in spherical droplets of 1400 water molecules. Protein and solvent are idealized as a series of concentric, spherical, dielectric media. Analysis results depend strongly on the treatment of the charged protein side chains at the protein/solvent interface. If charged side chains are viewed as part of the protein medium, then the protein dipole fluctuations are dominated by large, mutually uncorrelated, anisotropic, motions of the charged side chains. It is then incorrect to view the protein region as a single, homogeneous dielectric material. If one does take this view, estimates of the protein "dielectric constant" vary from 16 to 37, depending on the exact choice of model parameters. In contrast, if the charged portions of the charged side chains are viewed as part of the solvent medium, then theory and simulation are consistent: the protein dipole fluctuations excluding charged side chains are roughly those of a homogeneous, isotropic dielectric medium, with a dielectric constant of 4.7 ± 1.0 (ferro) or 3.4 ± 1.0 (ferri), in agreement with powder experiments. Statistical uncertainty and sensitivity to model parameters are small. Analysis of the radial dependence of the dipole fluctuations suggests that the inner half of the protein has a somewhat lower dielectric constant of 1.5–2, consistent with its biological function in electron transfer. These results suggest that Poisson–Boltzmann models could treat the protein bulk as a low-dielectric medium and the charged surface groups as part of the solvent region.**

The dielectric properties of proteins are central to their stability and activity (1). They make themselves felt in many ways. The low polarizability of the protein interior, for example, makes charge burial prohibitive and destabilizes point mutations that introduce net charges or dipoles within the molecule (2). The kinetics of charge transfer or charge separation steps in enzymatic reactions are influenced by the local dielectric properties in the active-site region, so that segregation of enzyme active sites from high-dielectric bulk solvent and preorganization of sufficiently rigid polar groups there are general constraints on enzyme structure (3, 4).

The general description of a protein's dielectric properties is a formidable problem. The static dielectric properties of a folded protein can be characterized on a microscopic level by a $3n \times 3n$ susceptibility tensor (5, 6), where n is the number of protein atoms. This tensor measures the response of the protein to an arbitrary perturbing charge density in the linear response limit. In the framework of continuum electrostatics, the problem is vastly simplified; the dielectric properties are characterized by a 3×3 susceptibility tensor, which can be obtained by summing the matrix elements of the microscopic susceptibility tensor. The continuum model has considerable practical importance, since it is being widely applied to macromolecules. To view a protein as a bulk dielectric, albeit with the experimentally observed shape and distribution of permanent charges, is obviously a severe approximation. In particular, substantial dielectric inhomogeneity and nonlinearity have been seen in protein simulations (5–8). The continuum model nevertheless reproduces solvation free energies of small molecules fairly well (9, 10) and has proven useful in protein modeling (11).

The protein macroscopic susceptibility can be estimated in several ways. Measurements on protein powders are the most direct approach, giving a static dielectric constant in the range of 2–5 for several proteins (12, 13). However, the protein charge distribution in these powders, and hence the dielectric response, will be very different from that in aqueous solution, since the ionizable residues (Asp, Glu, Arg, Lys, and His) will almost certainly all be in their neutral form. Organic molecules are possible model systems: polyamide crystals have a static dielectric constant of about 5 (14).

Finally, computer simulations can be used in conjunction with the Fröhlich–Kirkwood theory of dielectrics (15). The theory can be implemented in several ways. The protein can be viewed as an infinite homogeneous medium (16, 17) or as a finite sphere embedded within another dielectric material (vacuum or solvent) (5, 6, 8, 18). The dipole fluctuations can be obtained from microscopic simulations at various levels of sophistication. Long simulations of proteins in solution remain costly. Nevertheless, with rapidly advancing computer technology, this approach becomes increasingly attractive.

Here we implement the Fröhlich–Kirkwood theory for a material made of several concentric spherical shells. This could be a roughly spherical protein within a region of explicit solvent and a surrounding vacuum, for example. Other possible applications are layered clusters or micelles. This implementation will allow us to distinguish different layers within the protein, and within the solvent, all of which may have different dielectric properties. The treatment of the charged protein side chains is of particular importance. Two very different pictures emerge depending on whether these are viewed as part of the inner protein medium or as part of the outer solvent medium.

We analyze two 1-ns molecular dynamics simulations of ferro- and ferricytochrome *c* from yeast, solvated by 1400 water molecules and with spherical boundary conditions. Protein simulations with these boundary conditions are common (19). Cytochrome *c* itself is roughly spherical (20). We analyze the dipole fluctuations of the protein and their variations throughout the system. Simulations of a pure water droplet are analyzed for comparison.

MATERIALS AND METHODS

Theory. To derive the general expression for the dielectric constant, consider a system made of n concentric spherical

The publication costs of this article were defrayed in part by page charge payment. This article must therefore be hereby marked "*advertisement*" in accordance with 18 U.S.C. §1734 solely to indicate this fact.

†To whom reprint requests should be addressed.

regions, of dielectric constants $\varepsilon_1, \varepsilon_2, \ldots, \varepsilon_n$. The outer radius of region i is r_i; the outermost region n is infinite. We distinguish in each region a set of "low-frequency" degrees of freedom, which are ultimately to be simulated, and a set of "high-frequency" degrees of freedom, which form an underlying continuum of dielectric constant ε_i^{hf}. There is no loss of generality, since we are free to include all degrees of freedom in the low-frequency set. However, this distinction will be useful to interpret simulations including electronic polarizability.

Following Fröhlich (15), we can derive a fluctuation formula for the innermost region, 1, by introducing an applied field **E**, uniform far from the center of symmetry. A uniform cavity field F then reigns in region 1. **F** is obtained from elementary electrostatics (15) and has the form (21)

$$\mathbf{F} = f(\varepsilon_1, \varepsilon_2, \ldots, \varepsilon_n)\mathbf{E}. \quad [1]$$

In the three-medium case, for example,

$$f(\varepsilon_1, \varepsilon_2, \varepsilon_3) = \frac{9\varepsilon_2\varepsilon_3}{(\varepsilon_1 + 2\varepsilon_2)(\varepsilon_2 + 2\varepsilon_3) - 2(r_1/r_2)^3(\varepsilon_3 - \varepsilon_2)(\varepsilon_1 - \varepsilon_2)}. \quad [2]$$

The average polarization $\langle \Delta\mathbf{M}_{tot} \rangle$ in region 1 is along **E** and is given by

$$\langle \Delta\mathbf{M}_{tot} \rangle / V = \frac{\varepsilon_1 - 1}{4\pi}\mathbf{F} = \frac{\varepsilon_1 - 1}{4\pi} f(\varepsilon_1, \varepsilon_2, \ldots, \varepsilon_n)\mathbf{E}, \quad [3]$$

where V is the volume of region 1. If the applied field **E** oscillates with a high frequency, only the high-frequency polarization $\langle \Delta\mathbf{M}_{hf} \rangle$ develops:

$$\langle \Delta\mathbf{M}_{hf} \rangle / V = \frac{\varepsilon_1^{hf} - 1}{4\pi} f(\varepsilon_1^{hf}, \varepsilon_2^{hf}, \ldots, \varepsilon_n^{hf})\mathbf{E}. \quad [4]$$

The remaining polarization is termed the low-frequency polarization,

$$\langle \Delta\mathbf{M}_{lf} \rangle = \langle \Delta\mathbf{M}_{tot} \rangle - \langle \Delta\mathbf{M}_{hf} \rangle. \quad [5]$$

In region 1 we now view the low-frequency degrees of freedom microscopically, whereas the high-frequency degrees of freedom form an underlying continuum of dielectric constant ε_1^{hf}. The cavity field in region 1 is now $\mathbf{F} = f(\varepsilon_1^{hf}, \varepsilon_2, \ldots, \varepsilon_n)\mathbf{E}$. The microscopic degrees of freedom $\{X\}$ give rise to an instantaneous dipole moment $\Delta\mathbf{M}_{lf}(X)$. The interaction with **E** adds a term $\Delta\mathbf{M}_{lf}(X)\cdot\mathbf{F}$ to the potential energy. The Boltzmann average of $\Delta\mathbf{M}_{lf}(X)$, for small **E**, turns out to be

$$\langle \Delta\mathbf{M}_{lf} \rangle = \frac{\langle \Delta M_{lf}^2 \rangle_0}{3kT} f(\varepsilon_1^{hf}, \varepsilon_2, \ldots, \varepsilon_n)E. \quad [6]$$

$\langle\ \rangle_0$ indicates a Boltzmann average with $E = 0$. In all that follows we drop the subscript 0 for simplicity. From Eqs. **3–6** we obtain finally

$$\frac{\langle \Delta M_{lf}^2 \rangle}{kTr_1^3} = \frac{f(\varepsilon_1, \varepsilon_2, \ldots, \varepsilon_n)(\varepsilon_1 - 1) - f(\varepsilon_1^{hf}, \varepsilon_2^{hf}, \ldots, \varepsilon_n^{hf})(\varepsilon_1^{hf} - 1)}{f(\varepsilon_1^{hf}, \varepsilon_2, \ldots, \varepsilon_n)}. \quad [7]$$

If the inner region, 1, contains permanent charges, the previous derivation is only slightly modified. ΔM has simply to be interpreted as the deviation of the dipole moment from its mean.

$\langle \Delta M^2 \rangle$ is determined by the correlations between all pairs i, j of protein atoms:

$$\langle \Delta M^2 \rangle = \sum_{i,j} q_i q_j \langle \delta\mathbf{u}_i \cdot \delta\mathbf{u}_j \rangle, \quad [8]$$

where q_i is the partial charge of atom i and $\delta\mathbf{u}_i$ is its instantaneous displacement from its mean position.

The System and the Simulation. Two molecular dynamics simulations were performed, of yeast ferro- and ferricytochrome *c* (abbreviated 1YCC and 2YCC, respectively), solvated by 1400 TIP3P waters (22) at 293 K (23), starting from the crystal structures (20) and lasting 1 ns each. The last 900 ps were used for analysis. Electrostatic interactions were truncated beyond 12 Å (1 Å = 0.1 nm). The CHARMM/PARAM19 empirical force field was used (24). A soft spherical boundary potential (25) of radius 24 Å was used to confine the system. Simulations were done with the program X-PLOR (26).

Truncation of electrostatic forces in the simulations will affect the dipole fluctuations and, therefore, the estimated dielectric properties (27). While this effect is certainly significant, test simulations with a different cutoff (Fig. 1), and previous studies (28), suggest that it should not affect our results qualitatively.

The system can be idealized as a spherical protein surrounded by a spherical shell of water that is itself surrounded by a vacuum. We arbitrarily take the protein radius equal to $(5/3)^{1/2}$ times the radius of gyration, giving a hypothetical sphere that has the same radius of gyration as the real protein.

Simulations of a 24-Å droplet of pure water were carried out with the same protocol.

RESULTS

Protein Structure and Motion. Yeast cytochrome *c* is highly polar, with 38 charged groups out of 108 residues. The crystal structures of 1YCC and 2YCC are nearly identical (20). The rms deviation from the x-ray structure increased slowly in the 1YCC simulation, reaching 2.2 Å for all heavy atoms after 1 ns; it was stable at 1.9 Å throughout the 2YCC simulation. The protein remained fully solvated, near the center of the boundary sphere. The rms displacements around the mean structure were 0.5 Å on average in the interior and 1 Å for surface residues. Approximately 20 water molecules were bound to the protein throughout each simulation, mostly occupying clefts at the protein surface. The effective protein radius was 16.5 Å, with or without the bound waters. When the charged portions of the charged side chains (e.g., the ammonium group

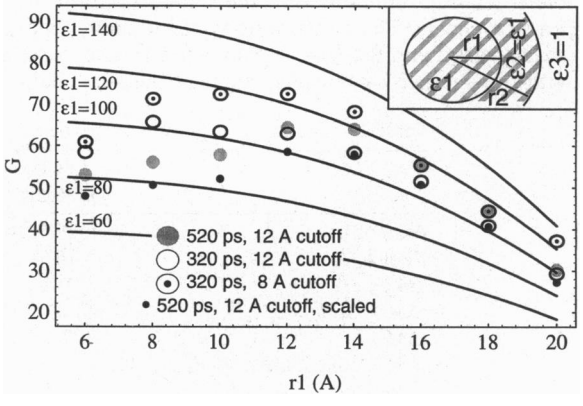

FIG. 1. *G* factor of the inner portion of a sphere of 1963 water molecules as a function of its radius r_1. Two simulation lengths and two cutoffs are compared (see text). Solid lines, continuum prediction for a series of dielectric constants ε_1; small dots: "scaled" *G* factor—i.e., each *G* value is divided by the water density within the inner region (thus normalizing the result to the density of bulk water). (*Inset*) Geometry of the system. The outer radius of the sphere is r_2 = 24 Å. The inner and outer solvent regions have the same dielectric constant, $\varepsilon_1 = \varepsilon_2$.

of lysine) were viewed as part of the outer, solvent region, then the effective radius of the protein region was reduced to 15.9 Å.

The radial distribution and the angular correlations of the water surrounding the protein were similar to those of the pure water droplet. However, the droplet exhibited an exaggerated density at its center (1.1 g/cm^3), as in previous work (25), due to surface tension. It had a large dielectric constant (≈110; see Fig. 1) as a result.

Protein Dipole Fluctuations. The system can be idealized as a spherical protein surrounded by a spherical shell of water, itself surrounded by a vacuum. The treatment of the charged side chains is particularly important, and in what follows we compare two approaches. The first is to view the entire protein as a single dielectric medium; the second is to exclude the charged portions of the charged side chains from the inner, "protein" medium, viewing them instead as part of the outer, "solvent" medium.

With this idealization, the protein's dielectric constant is determined by its dipole fluctuations through the so-called G factor (Eq. 7),

$$G = \langle \Delta M^2 \rangle / kTr_1^3. \quad [9]$$

When charged side chains are excluded from the analysis, we find $\langle \Delta M^2 \rangle = 23.9 \pm 3$ (eÅ)^2 for 1YCC and 15.8 ± 2 (eÅ)^2 for 2YCC; the G factors are 3.6 for 1YCC and 2.3 for 2YCC. The dipole fluctuations are roughly isotropic (Table 1), consistent with the picture of a homogeneous, isotropic dielectric medium. When charged side chains are included, we find $\langle \Delta M^2 \rangle = 127 \pm 7$ (eÅ)^2 for 1YCC and 132 ± 6 (eÅ)^2 for 2YCC; the G factors are 15.9 and 16.6. The dipole fluctuations are very anisotropic in this case (Table 1). Clearly, the properties of the protein bulk and those of its charged surface are very different.

In Eq. 8, we decomposed $\langle \Delta M^2 \rangle$ into a sum over correlations between pairs of protein atoms i, j. Using this decomposition, we can distinguish the following contributions to $\langle \Delta M^2 \rangle$: ($a$) self-correlations of the charged side chains, (b) cross correlations between charged side chains, (c) correlations of charged side chains with the protein backbone and with uncharged side chains, and (d) correlations of backbone atoms and uncharged side chains with each other. The self-correlation term due to the side chain of residue R, for example, is simply $\Sigma_{i,j \in R} q_i q_j \langle \delta \mathbf{u}_i \cdot \delta \mathbf{u}_j \rangle$, where the sum is over the side chain atoms of residue R. The other terms are defined similarly. Results are in Table 1: $\langle \Delta M^2 \rangle$ is dominated by the self-correlations of the charged side chains. The contributions of individual charged side chains vary from 0.2 (eÅ)^2 to 11.5 (eÅ)^2, and correlate well with the average rms displacement of the side chain.

Including the ≈20 ordered waters as an integral part of the protein increases $\langle \Delta M^2 \rangle$ only slightly: from 132 to 135 (eÅ)^2 for 2YCC with all side chains, and from 15.8 to 17.5 (eÅ)^2 for 2YCC excluding charged side chains.

Estimates of the Protein Dielectric Constant. The dielectric constant can be estimated from $\langle \Delta M_{tot}^2 \rangle$ by using Eq. 7. We first apply this approach to a 24-Å spherical droplet of pure water. The inner part of the droplet forms region 1, the outer part forms region 2, and the surrounding vacuum forms region 3. Fig. 1 shows the G factor of the inner region as a function of its radius r_1, as well as the prediction of continuum theory for a series of dielectric constants. The data follow the continuum prediction approximately but correspond to a large dielectric constant of 100–110. This is partly due to the large density in the inner part of the simulation sphere, which is a result of surface tension (25). Changing the cutoff distance affects G strongly for $r_1 \leq 12$ Å, but weakly for $r_1 \geq 16$ Å.

Despite surface tension effects, the boundary conditions used have been shown to give protein fluctuations in agreement with periodic boundary simulations (19, 29). Furthermore, the calculated protein dielectric constant will be shown to be very weakly sensitive to the solvent dielectric constant ε_2.

Applying Eq. 7 to cytochrome c, we assume $r_1 = 16.5$ Å (or 15.9 Å, if charged side chains are excluded from the inner region), $r_2 = 23$ Å (based on the radial profile of water density), and $\varepsilon_2 = 80$. The model contains three dielectric regions: the protein forms the inner region, 1; the solvent forms an intermediate region, 2; and the surrounding vacuum forms region 3. We compare two treatments of the charged protein side chains. The first views them as part of the inner, "protein" region. We then obtain $\varepsilon_1 = 24$ for 1YCC and $\varepsilon_1 = 25$ for 2YCC. This is close to earlier estimates for two other proteins (18). From the analysis in the preceding paragraph, we see that this dielectric constant is mainly related to mutually uncorrelated motions of the charged side chains. The second treatment views the charged portions of these side chains as part of the intermediate, "solvent" region. We then obtain $\varepsilon_1 = 4.7$ for 1YCC and $\varepsilon_1 = 3.4$ for 2YCC. These results are very weakly sensitive to the value of ε_2.

Treating the 20 ordered waters as an integral part of the protein increases ε_1 by 0.3 (charged side chains excluded).

Experimentally, completely dry cytochrome c powders have a dielectric constant of 3.6 ± 0.1. Water contents of 25, 50, and 100 water molecules per protein molecule increase the dielectric constant to 3.9, 4.6, and 6.1, respectively (13).

The calculated dielectric constant ε_1 is sensitive to the model parameters r_1, r_2, and ε_2, which are not uniquely defined, and to $\langle \Delta M^2 \rangle$, which contains statistical uncertainty. Fig. 2 illustrates the theoretical dependence of ε_1 on all these param-

Table 1. Summary of protein properties

	1YCC, all atoms*	2YCC, all atoms*	1YCC, uncharged†	2YCC, uncharged†
Axes of inertia, Å	13.7, 19.3, 16.1		12.8, 18.6, 14.9	
Radius, Å	16.5	16.5	15.9	15.9
$\lvert\langle \mathbf{M} \rangle\rvert$‡, eÅ	141	162	179	199
$\langle \Delta M_x^2 \rangle$, $\langle \Delta M_y^2 \rangle$, $\langle \Delta M_z^2 \rangle$§	37, 20, 70	36, 25, 71	9, 7, 8	7, 5, 4
$\langle \Delta M^2 \rangle$	127 ± 7	132 ± 6	23.9 ± 3.0	15.8 ± 2.0
$\langle \Delta M^2 \rangle$, contributions a–d¶	123, −2, −18, 24	100, 13, 4, 19		
G factor	15.9	16.6	3.6	2.3
ε	24 ± 10	25 ± 10	4.7 ± 1.0	3.4 ± 1.0
Experimental ε‖			3.6–4.6	

Dipole moments are in eÅ.
*Results including all protein atoms.
†Results excluding charged side chains.
‡Magnitude of mean dipole moment.
§Variances of dipole components along each cartesian axis.
¶Contribution of different types of correlations to $\langle \Delta M^2 \rangle$ (see text).
‖From ref. 13, with 0–50 bound water molecules.

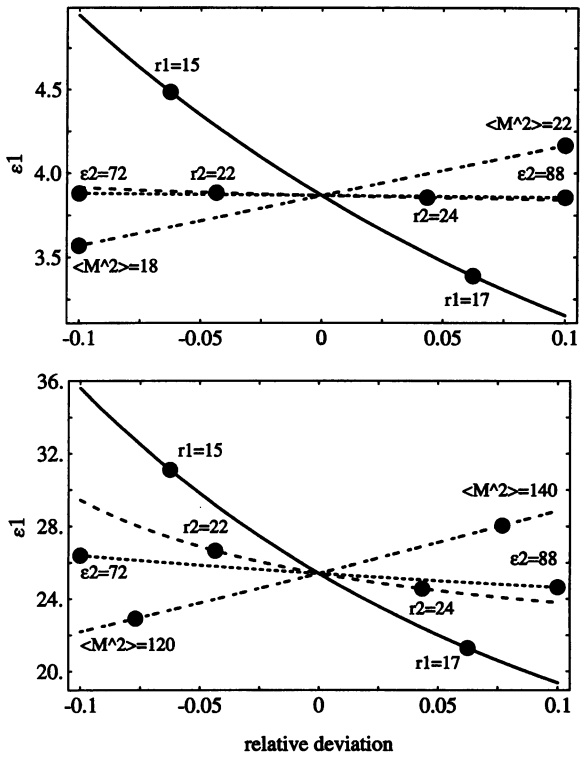

FIG. 2. Theoretical dependence of ε_1 on r_1, r_2, ε_2, and $\langle \Delta M^2 \rangle$. Parameter variation is measured by relative deviation from the central values $r_1 = 16$ Å, $r_2 = 23$ Å, $\varepsilon_2 = 80$, and $\langle \Delta M^2 \rangle = 20$ (eÅ)^2 (*Upper*) or $\langle \Delta M^2 \rangle = 130$ (eÅ)^2 (*Lower*). Each curve corresponds to the variation of one parameter and is labeled by two representative points.

eters, varying them over a reasonable range around the points $r_1 = 16$ Å, $r_2 = 23$ Å, $\varepsilon_2 = 80$, and $\langle \Delta M^2 \rangle = 20$ (eÅ)^2 (typical of the protein without charged side chains) or $\langle \Delta M^2 \rangle = 130$ (eÅ)^2 (typical of the protein with all side chains). The most critical parameter appears to be the protein radius r_1. When charged side chains are included in the protein region, estimates of ε_1 range from 16 [$r_1 = 17$ Å, $r_2 = 24$ Å, $\varepsilon_2 = 110$, $\langle \Delta M^2 \rangle = 120$ (eÅ)^2] to 37 [$r_1 = 15$ Å, $r_2 = 23$ Å, $\varepsilon_2 = 70$, $\langle \Delta M^2 \rangle = 140$ (eÅ)^2], giving an uncertainty on the order of ± 10 units. ε_1 is very insensitive to ε_2.

When charged side chains are excluded from the inner protein region, the sensitivity of ε_1 to the model parameters is greatly reduced. Estimates of ε_1 then range from 2.9 to 5.3.

Radial Variation of the Protein Dielectric Constant. We now divide the protein itself into two regions: we view the inner part as a microscopic cavity, whose dielectric constant ε_1 will be derived from its dipole fluctuations, and the outer part as a continuum (Fig. 3*a*). By varying the radius r_1 of the inner region, we can analyze the radial variation of the protein dielectric constant.

We must, however, make an assumption about the dielectric constant of the outer portion of the protein, ε_2. We can assume for example that the two protein regions have the same (unknown) dielectric constant, $\varepsilon_1 = \varepsilon_2$. Or we can set ε_2 equal to the overall protein dielectric constant obtained in the previous paragraph, $\varepsilon_2 = 24$–25. These two assumptions tend respectively to underestimate and to overestimate the theoretical G.

The theoretical G is plotted in Fig. 3*b* as a function of r_1 for several values of ε_1 (with the assumption $\varepsilon_1 = \varepsilon_2$; results with $\varepsilon_2 = 25$ are similar). Numerical results from the simulation are superimposed. When charged side chains are excluded from the protein regions, the observed G factor varies smoothly with r_1. For $r_1 \geq 12$ Å, it follows approximately the theoretical curve corresponding to $\varepsilon_1 = 3$–3.5. For $r_1 \leq 10$, it follows the curve

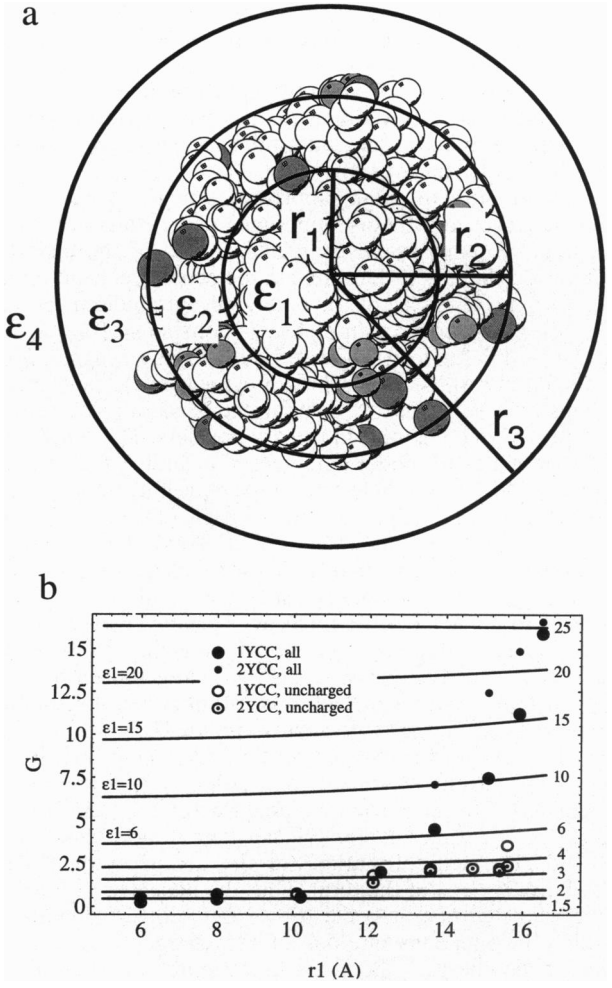

FIG. 3. (*a*) Geometry of the four concentric dielectric regions. Charged groups are gray. (*b*) G as a function of r_1, with and without charged side-chain contributions. Theoretical curves are labeled by the value of the inner dielectric ε_1.

$\varepsilon_1 = 1.5$–2. Thus, the dielectric constant of the protein decreases in the inner part of the molecule, which is less polar and mobile than the exterior. This is consistent with the requirement of a low reorganization free energy for charge transfer to and from the heme (5).

When charged side chains are included in the protein regions, the observed G values increase sharply as r_1 increases from 12 to 16.5 Å. The corresponding dielectric constant increases from the internal value of 1.5–3, up to 24–25.

CONCLUSION

We have used Fröhlich–Kirkwood theory to analyze two long molecular dynamics simulations of cytochrome *c*, with 1400 explicit water molecules and spherical boundary conditions. The protein is viewed as one or more spherical dielectric media, characterized by their macroscopic dielectric constants. With this spherical idealization, the protein dielectric constant is simply related to its mean square dipole fluctuations.

Details of truncation and boundary conditions should not affect our results qualitatively. While the boundary conditions do affect the water density (25) and dielectric constant (Fig. 1), they are known to give protein fluctuations in good agreement with periodic boundary simulations (19, 29). The spherical geometry allows us to treat the electrostatic boundary conditions rigorously, and the theoretical protein dielectric constant is very insensitive to the exact solvent dielectric constant ε_2.

The probability distribution of the protein's ΔM^2 from the simulations (not shown) agrees with a recent continuum prediction (30); and the solvent reaction field at the protein center is within 50% of the continuum prediction. Furthermore, simulations of two other proteins with periodic boundary conditions and different truncation schemes gave a similar ε_1 (with all side chains) (18).

Although the continuum approximation is severe at the molecular level, the theory and simulation results are fairly consistent, as long as the charged portions of the charged protein side chains, concentrated at the protein/solvent interface, are viewed as part of the outer, solvent medium. In this case, our estimated protein dielectric constants of 4.7 ± 1.0 and 3.4 ± 1.0 for ferro- and ferricytochrome *c* agree with experimental results on powders of cytochrome *c* (and other proteins). These should be comparable, since all side chains are expected to be neutral in the dry powders. The sensitivity of our estimates to model parameters, including the protein radius and the solvent dielectric constant, is fairly modest; the dipole fluctuations are reasonably isotropic (Table 1); and the statistical uncertainty of $\langle \Delta M^2 \rangle$ is small. Analyzing the radial variation of ε_1, it appears that two regions can be distinguished within the protein. The innermost region, made up of atoms less than 10–11 Å from the molecule's center, behaves like a homogeneous medium with a dielectric constant of 1.5–2. The remaining, outer region has a slightly higher dielectric constant, so that the total dielectric constant is 3.4–4.7 for the whole protein (charged side chains excluded).

The behavior of the charged protein side chains, located at the protein/solvent interface, is very different from that of the protein bulk. The mean square dipole fluctuation $\langle \Delta M^2 \rangle$ of the protein is 5–8 times larger when charged side chains are included. The self-correlations of the charged side chains contribute 75–95% of the total. Thus the dielectric relaxation of the whole protein in a perturbing field consists mainly of mutually independent motions of the charged side chains. Some of the charged side chains contribute almost as much individually to $\langle \Delta M^2 \rangle$ as all the uncharged side chains together. The anisotropy of $\langle \Delta M^2 \rangle$ is also very large. It is thus difficult to view the entire protein, charged side chains included, as a single, homogeneous, isotropic dielectric medium. If one does take this view (18), the estimated dielectric constant is highly sensitive to the model parameters, with estimates ranging from 16 to 37 in our case, depending on the model parameters.

This suggests that Poisson–Boltzmann models (11) could treat the protein bulk as a low-dielectric medium and the charged surface groups either as part of the solvent region (e.g., ref. 31) or as another, intermediate, region.

Simulations were done on the Cray YMP-C98 computer of the Centre National de la Recherche Scientifique.

1. Perutz, M. (1978) *Science* **201,** 1187–1191.
2. Richards, F. & Lim, W. (1994) *Q. Rev. Biophys.* **26,** 423–498.
3. Krishtalik, L. (1980) *J. Theor. Biol.* **86,** 757–777.
4. Warshel, A. & Russell, S. (1984) *Q. Rev. Biophys.* **17,** 283–342.
5. Simonson, T., Perahia, D. & Bricogne, G. (1991) *J. Mol. Biol.* **218,** 859–886.
6. Simonson, T., Perahia, D. & Brünger, A. T. (1991) *Biophys. J.* **59,** 670–690.
7. Simonson, T. & Perahia, D. (1992) *Biophys. J.* **61,** 410–427.
8. King, G., Lee, F. & Warshel, A. (1991) *J. Chem. Phys.* **95,** 4366–4377.
9. Sitkoff, D., Sharp, K. & Honig, B. (1994) *J. Phys. Chem.* **98,** 1978–1988.
10. Simonson, T. & Brünger, A. T. (1994) *J. Phys. Chem.* **98,** 4683–4694.
11. Sharp, K. & Honig, B. (1991) *Annu. Rev. Biophys. Biophys. Chem.* **19,** 301–332.
12. Bone, S. & Pethig, R. (1982) *J. Mol. Biol.* **157,** 571–575.
13. Bone, S. & Pethig, R. (1985) *J. Mol. Biol.* **181,** 323–326.
14. Baker, W. & Yager, W. (1942) *J. Am. Chem. Soc.* **64,** 2171–2177.
15. Fröhlich, H. (1949) *Theory of Dielectrics* (Clarendon, Oxford).
16. Gilson, M. & Honig, B. (1986) *Biopolymers* **25,** 2097–2119.
17. Nakamura, H., Sakamoto, T. & Wada, A. (1989) *Protein Eng.* **2,** 177–183.
18. Smith, P., Brunne, R., Mark, A. & van Gunsteren, W. (1993) *J. Phys. Chem.* **97,** 2009–2014.
19. Brooks, C., Karplus, M. & Pettitt, M. (1987) *Adv. Chem. Phys.* **71,** 1–259.
20. Berghuis, A. M. & Brayer, G. D. (1992) *J. Mol. Biol.* **223,** 959–976.
21. Powles, J., Fowler, R. & Evans, W. (1984) *Chem. Phys. Lett.* **107,** 280–283.
22. Jorgensen, W., Chandrasekar, J., Madura, J., Impey, R. & Klein, M. (1983) *J. Chem. Phys.* **79,** 926–935.
23. Berendsen, H., Postma, J., van Gunsteren, W., DiNola, A. & Haak, J. (1984) *J. Chem. Phys.* **811,** 3684–3690.
24. Brooks, B., Bruccoleri, R., Olafson, B., States, D., Swaminathan, S. & Karplus, M. (1983) *J. Comp. Chem.* **4,** 187–217.
25. Brünger, A. T., Brooks, C. L. & Karplus, M. (1984) *Chem. Phys. Lett.* **105,** 495–500.
26. Brünger, A. T. (1992) X-PLOR, A system for x-ray crystallography and NMR (Yale Univ. Press, New Haven, CT), Version 3.1.
27. Neumann, M. (1983) *Mol. Phys.* **50,** 841–858.
28. Loncharich, R. & Brooks, B. (1989) *Proteins* **6,** 32–45.
29. Brooks, C. & Karplus, M. (1989) *J. Mol. Biol.* **208,** 159–181.
30. Kusalik, P. (1993) *Mol. Phys.* **80,** 225–231.
31. Delepierre, M., Dobson, C., Karplus, M., Poulsen, F., States, D. & Wedin, R. (1987) *J. Mol. Biol.* **197,** 111–130.